Development of the marine Holocene environment in a drowned paleovalley with final anthropic influence in the Cartagena Bay (Murcia, SE Spain)

Trinidad Torres,[1] José E Ortiz,[1,*] Sebastián Ramallo,[2] Milagros Ros,[2] Yolanda Sánchez-Palencia,[1] Ana Blázquez,[3] Felipe Cerezo,[4] Ignacio López-Cilla,[5] Luis A Galán,[5] Ángeles G Borrego,[6] Blanca Ruiz-Zapata,[7] María José Gil,[7] Ignacio Manteca[8] and Tomás Rodríguez-Estrella[8]

[1]Laboratorio de Estratigrafía Biomolecular, E.T.S.I. Minas y Energía de Madrid, Universidad Politécnica de Madrid, Spain

[2]Departamento de Prehistoria, Arqueología, Historia Antigua, Historia Medieval y Ciencias y Técnicas Historiográficas, Universidad de Murcia, Spain

[3]Institute of Environment and Marine Science Research (IMEDMAR), Universidad Católica de Valencia, Spain

[4]Departamento de Historia, Geografía y Filosofía, Facultad de Filosofía y Letras, Universidad de Cádiz, Spain

[5]Departamento de Infraestructura Geocientífica y Servicios, IGME, Spain

[6]Instituto de Ciencia y Tecnología del Carbono (INCAR-CSIC), Spain

[7]Facultad de Ciencias, Universidad de Alcalá de Henares, Spain [8]Departamento de Ingeniería Minera, Geológica y Cartográfica, Universidad Politécnica de Cartagena, Spain

***Corresponding author:** José E Ortiz, Laboratorio de Estratigrafía Biomolecular, E.T.S.I. Minas y Energía de Madrid, Universidad Politécnica de Madrid, C/ Ríos Rosas 21, Madrid 28003, Spain. Email: joseeugenio.ortiz@upm.es

Abstract

Sedimentological, paleobiological, mineralogical, and geochemical analyses of a sediment core retrieved on the seafront of Cartagena Bay were performed after high-resolution sampling. A wide series of dates obtained through radiocarbon and amino acid racemization proved that the Holocene record on the analyzed core began at ca. 7300 yr cal BP. Reinterpretation of the marine seismic profiles indicated that the beginning of this transgression was channeled along erosive paleochannels excavated on a coastal plain of, at least, MIS5c age. The Holocene paleoenvironmental evolution consisted of a first period marked by marine conditions with strong inputs from a fan delta linked to the reorganized fluvial network that occurred after the sudden rise of the base level, which caused a growing sedimentary prism. Later, the full marine environment was reflected in the development of a *Posidonia-Cymodocea* meadow hosting a rich biodiversity of marine species (mollusks, foraminifera, ostracoda). Around 3800 yr cal BP, the area underwent a profound change and a silting process started to alter the conditions, turning the area into a paucispecific brackish marsh environment in which mud deposition was dominant. Since Carthaginian times, arrangement works locally affected the record, allowing the arrival of some marine species due to port work (dredging) undertaken to gain depth and showing anthropic influence.

Keywords

landscape changes, magnetic susceptibility, mineralogy, paleobiology, Punic and Roman port works, sedimentology

Received 27 September 2021; revised manuscript accepted 14 January 2022

Introduction

Cartagena Bay (Murcia, Spain) is one of the most interesting areas in the Mediterranean realm as it reflects the geographical evolution of this zone since the beginning of historical times. The bay is characterized by a richness of raw materials, such as iron, lead, and silver, as attested by old mines, tail ponds, slag heaps, and abandoned metallurgical factories (Bode et al., 2015; Domergue, 1990; Ramallo and Berrocal, 1994; Trincherini et al., 2009). The abundant wealth of the area brought about the growth of the city of Cartagena via terracing, landfill, and reclamation processes, to such an extent that outcrops were almost absent.

The protected bay is considered the most perfect natural anchorage along the coast of Spain. During Roman times, docks were built, and piers and related warehouses can still be observed buried below 19th-century buildings, thereby attesting to the artificial retreat of the waterline. Later, a galley base was established and there was continuous development of navy facilities from the 18th century onward, reflected by the city wall and development of docks, shipyards, and arsenals, as well as increasing and continuous dredging processes (Conesa and García-García, 2003; Pérez-Crespo, 1992). Finally, population growth in Cartegena led to the expansion of the city beyond its walls, with settlement sprawling toward the north and covering the marsh of El Almarjal. The characteristics of the area imply that the interplay between eustasy, paleo-landscape, neotectonics, and anthropic activity hinders research into its recent geological record on land.

In 2017, an excavation was made to rebuild a 19th-century building named “Tivoli.” An interesting Holocene section cropped out at the foundation wall (named E1), revealing a coastal character, with black muds with drifted *Posidonia oceanica* remains and articulated shells at the bottom, followed by fine sands with pelecipoda shells, and sands with pottery shreds and logs driven into the sediments in the uppermost part, thus indicating its use during Punic times (Torres et al., 2018). In addition, the remains of a Roman mole are still visible in another historical building named Casa Llagostera Foundation (E2), close to E1 section (Figure 1).

Sixteen boreholes with continuous core recovery on building plots and gardens were obtained on works conducted by teams from the University of Murcia (Manteca et al., 2017; Torres et al., 2018). Together with technical reports from tens of geotechnical drill holes in the area, these boreholes allowed a general paleoen- vironmental reconstruction (Torres et al., 2018) mostly focused on marsh deposits inland (El Almarjal) and therefore poorly representing typical marine deposits.

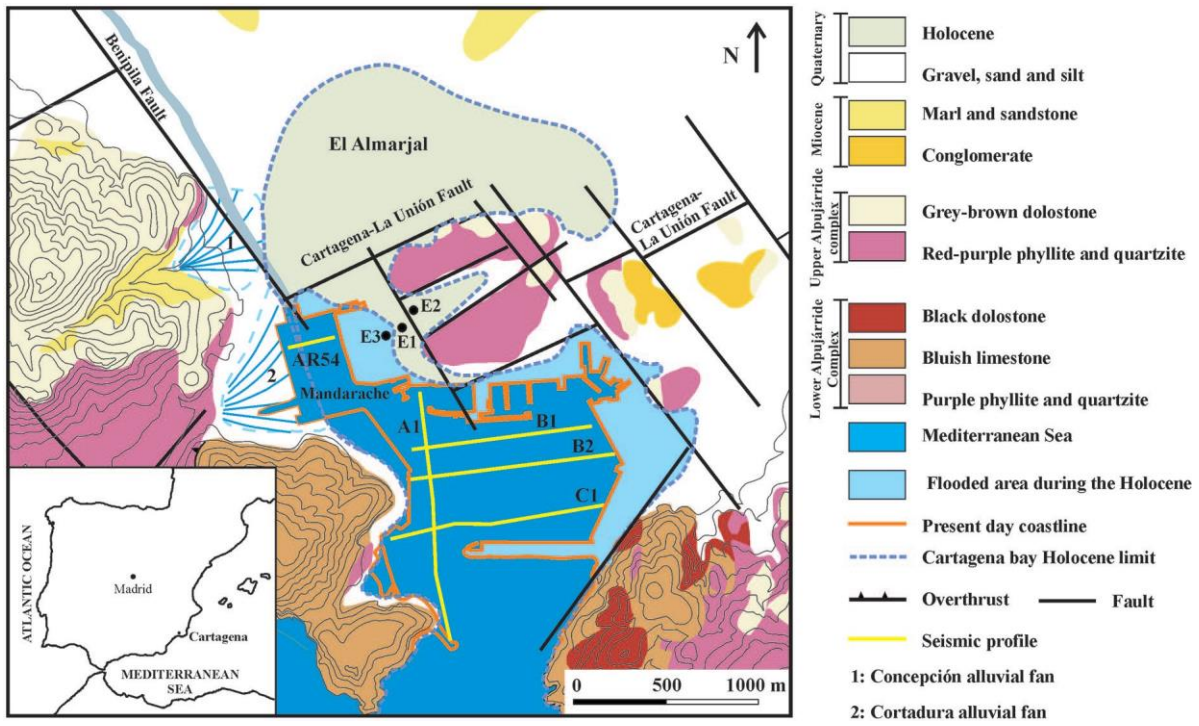

Figure 1. Geographical location of Cartagena. Geological map (modified from Manteca et al., 2017) with the location of the seismic profiles shown in Figure 2.

To better understand the evolution of the basin and the paleoenvironmental characteristics of the coastal margin during the Holocene, including the human activities that influenced sedimentation in historical times (Punic and Roman epochs), we drilled a new core (E3) in the vicinity of E1 and Casa Llagostera (E2) (Figure 1). Of note, E3 contains a well preserved and large record covering the whole Holocene record (11.1 m), which was dated through radiocarbon and amino acid racemization (Ortiz et al., 2021), thus allowing continuous sampling (with 3 cm inter- vals) for a high-resolution study. Furthermore, intense amino acid racemization and radiocarbon sampling followed by a Bayesian analysis allowed the establishment of a reliable chronology (Ortiz et al., 2021).

To this end, we performed a multidisciplinary study of the paleoenvironmental evolution considering the sedimentological characteristics, paleontological content, mineralogy, and trace elements together with a reinterpretation of geophysical data. Thus, this study aimed to reconstruct the paleoenvironmental conditions and the landscape evolution of Cartagena Bay over the Holocene and the influence of human settlements.

Geographical and geomorphological settings

Cartagena Bay is an estuarine environment enclosed by craggy sierras – La Muela-Atalaya and La Fausilla, among others – that protect it from dominant easterly winds. To its north, the hills where Punics and Romans built their cities, act as a partial lock that separate them from a wide marsh 2 m

above the sea level, El Almarjal (Figure 1), which, after intensive drainage, is now covered by buildings.

An ephemeral stream, named Benipila Creek, with a catchment area of 72.5 km^2 (Conesa and García-García, 2003) runs along the southern boundary of El Almarjal marsh debouching at the southern corner of the bay at the "Mar de Mandarache," where navy facilities were built. Other minor streams, which are wadis, built the small alluvial fans of Concepción and Santa Lucia, as well as a number of minor ones that now reach the bay through the sewage system.

The underwater environment of Cartagena Bay holds a fossilized paleo-landscape excavated on soft sediments of a coastal plain of MIS5 age, as revealed by marine geophysics (Cerezo, 2016; Torres et al., 2018, 2020). This landscape conditioned the inflow of marine water during MIS1, as discussed later. From a geological perspective, the present morphology of the study area was developed during the Alpine Orogeny, which stacked a series of nappes of metamorphic rocks belonging to both the Nevado-Filabride Complex and the Alpujárride Complex (Figure 1). The Cartagena-La Unión Fault, separates the meta- morphic complexes from a large depression named "Campo de Cartagena" with a thick Neogene infill that shows only slight deformation (Manteca Martínez and García García, 2004). A fault network of NW-SE and NE-SW (N.70 and N.130) strike controlled the course of Benipila Creek (Benipila Fault) and the morphology of El Molinete Hill. In the area iron, lead, copper, and silver ores accumulated from hydrothermal processes linked to volcanic calco-alkaline activity during the Neogene (Manteca Martínez and Ovejero Zappino, 1992; Oen et al., 1975).

Material and methods

Drilling and sampling

We drilled a 30-m-long core with a diameter of 7 cm named E3, which was obtained with a conventional single barrel drill pipe and continuous core recovery (95%) with a direct flow of water. The core boxes were stored under controlled conditions in a wet chamber. For sampling, the core surface was scraped to remove any contamination linked to the drilling process. The soft sediments were manually split into two halves using a steel blade. One half was stored at the Spanish Geological Survey facilities for further study, while the other half was sampled by driving plastic boxes ($3 \times 3 \times 1$ cm) into it.

The uppermost 3.1 m consisted of very recent rubble (19^{th} century) and encaustic cement tile fragments. This rubble was used as infill for this swampy area and was discarded for the purposes of this study.

The chronology between 11.1 and 3.1 m was obtained through radiocarbon dating (10 samples) and amino acid racemization of ostracoda (30 ostracoda valves from 12 beds) (Ortiz et al., 2021). The chronology established revealed that materials of the upper

11.1 m belonged to the Middle (8300–4200 yr BP or Northgrippian) and Upper (>4200 yr BP

Meghalayan) Holocene stages. A chronological model for MIS1 was constructed with the Bayesian R-code package "Bacon 2.3.7" (Blaauw and Christen, 2011) after 9000 Markov Chain Monte Carlo iterations. The record between 11.1 m and the bottom of the core was dated at MIS5c.

A total of 216 representative samples with a thickness of 1 cm were taken at ca. 3 cm intervals between 11.1 and 3.1 m, each sam- ple being separated into diverse subsamples for different studies: sedimentology and paleontology; X-Ray fluorescence (XRF); X-ray diffraction (XRD); and magnetic susceptibility (MS).

Sedimentology and paleontology

To examine the sedimentological and paleontological content, samples of ca. 100 g were dried at room temperature and water- dispersed. They were then passed through a 63-μm sieve, dried, and weighed to calculate the mud fraction. Examination under a microscope allowed determination of the textural and microfossil content.

Given the low weight of the dry sample, the frequency of macro-mollusk species was considered unsuitable for statistical analyses. Therefore, we focused on micro-mollusks, which were counted in all the samples and normalized their frequency to 100 g.

Mollusks and microfossils (foraminifera, ostracoda) were identified at species level and exceptionally at genus level. For the identification of mollusk species, we used Arduino et al.'s (2016) web page and data from the studies by Giannuzzi–Savelli et al. (1997) and D'Angelo and Gargiullo (1978).

To identify ostracoda species, we used the studies of Carbonel (1985), Guillaume et al. (1985), Mazzini et al. (1999), Nachite et al. (2010), and Martínez-García et al. (2013).

To identify benthic foraminifera, we followed Loeblich and Tappan (1988), Milker and Schmiedl (2012), Hayward et al. (2017), and WORMS (Word Register of Marine Species/World Foramin- ifera Database). The Density index is calculated by the number of carapaces per g. The Shannon-Weaver diversity index allows estimation of specific diversity by taking into account the number of individuals and also the number of taxa (Spellerberg and Fedor, 2003). This index is defined by $H = \sum[(pi) \times \ln(pi)]$, where pi is the proportion of total sample represented by species i, and it is calculated by dividing the number of individuals of species i by the total number of samples. The Fisher's alpha index is another diversity proxy that establishes the relationship between the number of species and the number of individuals of those species (Fisher et al., 1943). It is defined implicitly by the formula $S = \alpha \times \ln(1 + n/\alpha)$, where S is number of taxa, n is number of individuals, and α is the Fisher's alpha. The Equitability index is a function of species even- ness and it takes into account the number of species and the relative abundance of species in a community (Begon et al., 1996). It is calculated using the Shannon-Weaver diversity index divided by the logarithm of the number of taxa ($E = H/\log(S)$).

Mineralogical analysis by X-Ray Diffraction (XRD)

We selected 216 samples between 11.1 and 3.1 m and powdered them to <10 μm. The mineralogy of these samples was obtained with an XRD Rigaku MiniFlex 300/600 difractometer. An X-ray tube with Cu anode material was used as radiation source, with a Cu-Kα target tube. The primary divergent slit was 0.625° and the axial soller slit 1.25°. Scans were made over a 2Θ range of 10°–110° with a total exposure time of 14 min. For the regular powders, a step size of 0.05° and a counting time of 56.9 s/step were used.

Magnetic susceptibility

Magnetic susceptibility (MS) has recently been used to differenti- ate source areas in Late Quaternary deposits (Boar and Harper, 2002; Chan et al., 1998; Ghilardi et al., 2008; Robinson et al., 1995; Rowntree et al., 2017). Although the size and shape of mineral grains can lead to different responses to the measurements (Maher, 1998; Yim et al., 2004), we chose to use MS as it is a non-destructive – a valuable criterion due to sample scarcity.

MS reflects the capacity of a substance to be magnetized. In the case of rocks and sediments, it is also a measure of their ferromagnesian mineral content. This parameter can be used as a proxy of high-flow periods, that is to say, periods marked by an increase in the flux of detrital magnetite-bearing material. In addition, the magnetic particle content can be later modified depending on the oxidation/reduction processes that occur after sedimentation. Therefore, MS can also be used as a proxy of the extent of reductive iron oxide dissolution processes (Canfield and Berner, 1987; Dekkers, 1997; Murdock et al., 2013; Nowaczyk et al., 2004; Ortega et al., 2006).

Magnetic susceptibility (MS) data were obtained at the Spanish Geological Survey using the U-channels of a GEOTEK Multi-Sen- sor Core Logger (MSCL-GEOTEK) equipped with a Bartintong MS2E surface point sensor for MS determination. The resolution of the sensor is 2×10^{-6} SI on the 0.1 SI measurement range.

C, H, and N analysis

Another set of 216 samples along the uppermost 11.1-m-long section were taken for CHN analysis. These samples (1 g) were then homogenized with a mortar and pestle. The inorganic carbon fraction was removed by adding HCl. Total C, H, and N were determined using a LECO CHN-2000 analyzer (LECO Corp, St. Joseph, MI) at INCAR (CSIC).

Geophysics

A marine geophysical survey campaign was carried out in Cartagena Bay, the primary results of which were widely described in Cerezo (2016). The campaign was performed using a SES-2000 Parametric Sub-Bottom Profiler (sediment echosounder) with the specific software INNOMAR (SESWIN) and the Hydromagic/ Survey software for position control. The different tracks were oriented N-S along the major axis of the bay and perpendicular to it. Reinterpretation of the data is

presented on the basis of the new stratigraphical data observed in the E3 record, a series of fence diagrams, and a chrono-stratigraphical reassignment.

E1 section

We also obtained a manual core, named E1, from a 5.4-m-thick section in the foundations of a new building. This core was sampled for dating (^{14}C and AAR) and sedimentology and paleobiology analysis (Torres et al., 2018). New samples from the uppermost part were chosen for radiocarbon dating, and sedimentology and paleobiology were revised.

Radiocarbon dating

Seven new samples, consisting of plant and charred material, and wood, from various depths (Table 2) were sent to Beta Analytic for radiocarbon dating. An articulated marine shell found in life position was sent to the "Centro Nacional de Aceleradores" (CSIC, Seville, Spain).

Samples were pre-treated with diluted HCl and NaOH to remove carbonate and secondary organic acids, respectively. Finally, they were rinsed with acid to neutralize the solution before drying. The carbon in the samples was reduced to graphite (100%), which was then examined for ^{14}C content with an accelerator mass spectrometer. The radiocarbon age was calculated and calibrated using the CALIB 8.2 program (Stuiver et al., 2021) with the INTCAL20 calibration curve (Reimer et al., 2020) for the wood, plant, and charred material, and the MARINE20 calibration curve (Heaton et al., 2020) for the marine shell. All age values are in calibrated years BP (cal BP).

Results

Geophysics

For the fence correlation, five geophysical profiles reported by Cerezo (2016) were selected, one of them (A1) with an N-S align- ment and four (B1, B2, C1, and AR54) with an E-W orientation (Figure 2). Based on the stratigraphy of core E3, it was possible to gage the former seismostratigraphical units, namely the infill of the Holocene units and also the ancient thalweg, which represents a primary stage of the still active Benipila wadi before Holocene times. Taking into account the vertical scale of the graphs, the fluvial incision of the Upper Pleistocene age appears to have been only moderate, although a general areolar erosive surface without defined channels resulting from a stronger erosive process cannot be discarded. Thus, the Holocene record unconformably lies on an erosive surface developed over, at least, MIS5c coastal plain sediments – findings consistent with the information provided in previous drilling campaigns (Torres et al., 2018). The Holocene seismic unit consisted of a stratified lower bed capped by a mas- sive unit formed by recent ooze rich in organic matter, locally with anthropic influence.

It must be highlighted that in the Mandarache area (NE area of Cartagena Bay), the AR54 profile nicely marked the development of a fan delta at the mouth of the Benipila Creek or a minor alluvial

fan, the development of which was identified in Torres et al. (2018). Indeed, the activity of this creek is reflected in nearby cores, which showed alluvial fan deposits made of gravel beds.

The fence correlation also revealed paleo-channel infills that could hold a more complete Holocene marine record.

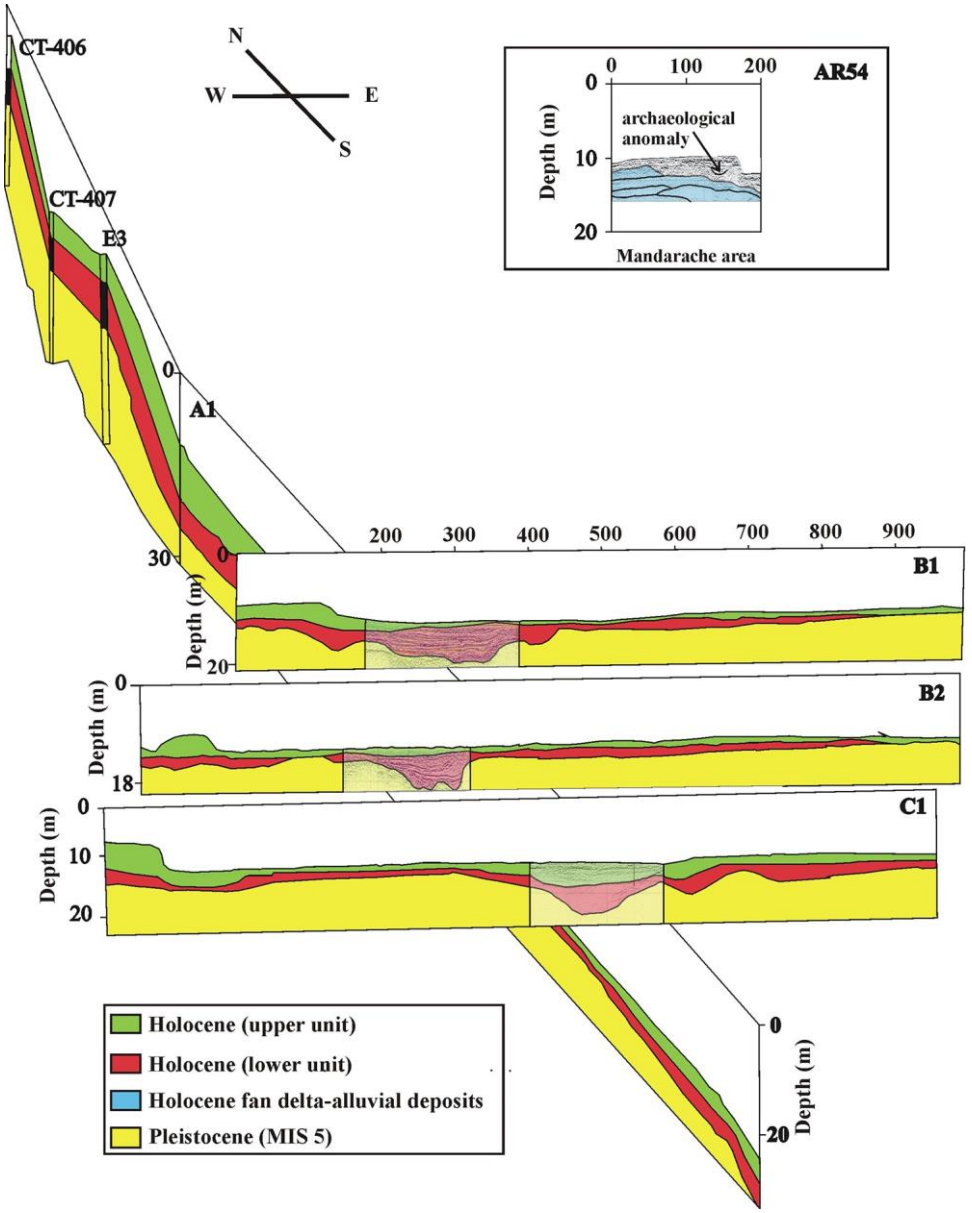

Figure 2. Fence correlation of seismic profiles A1, B1, B2, C1, and AR54. The single seismic profiles were modified from Cerezo (2016). Data from inland cores CT407, CT408, E1, and E3 sections are included. Seismic Units are described in the text, and the position of the seismic lines are shown in Figure 1. AR54 seismic profile is located at the NE area of Cartagena Bay and is not included in the general fence correlation.

Sedimentology and mineralogy

The Holocene record core showed mainly brown/gray to black muddy sands, sometimes with clearly recognizable marine plant remains and shell fragments, linked to reducing conditions. There were also medium-size sand beds, especially at the bot- tom, and some horizons of sandy muds (Figure 3). Generally speaking, the most abundant sediment size was between 63 µm and 2 mm (sand).

The mineral content was dominated by quartz (average: 40%), calcite (29%), dolomite (6%), and micas (20%), with significant amounts of clay minerals also present in some beds (Figure 3). Quartz usually corresponded to fine-grained sands, most likely derived from Miocene age sandstones that outcrop in the nearby catchment of the Benipila Creek. Calcite and aragonite were considered together because it was impossible to distinguish between grains of pure detrital origin and bioclastic particles (sometimes complete shells of micro-mollusk and foraminifera). Dolomite had a clear detrital origin and its source can be confidently placed in the mountains at each side of the bay where dolostone beds make up the major lithology. Mica group minerals and other silicate groups were linked to the micaceous siltstones of Miocene age, as well as to the micaceous schists of the catchment.

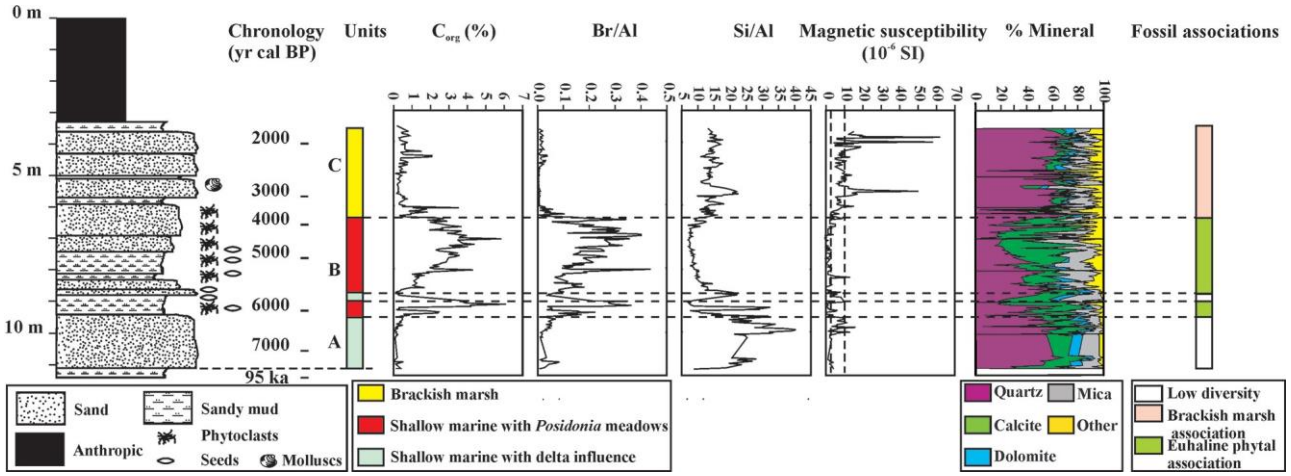

Figure 3. Stratigraphic section of the Holocene record of core E3 with the chronological scale (Ortiz et al., 2021), and the profiles of C_{org}, Br/Al, Si/Al (Ortiz et al., 2021), magnetic susceptibility, and predominant mineral components. The environmental interpretation based on mollusk, ostracoda, and foraminifera associations is included.

The mineralogical content showed scarce variations along the Holocene record, although certain changes allowed the differentiation of three intervals (Figure 3).

In interval A (11.1–8.7 m), quartz dominated (>60%), and calcite+ aragonite (10–15%) and dolomite were abundant. Mica minerals were frequent (10–15%). Shifts toward very low quartz percentages were detected at 9.7 and 9.4 m. A different case is a group of seven samples in the 9.2–9.0 m interval, which showed a marked decrease in the quartz content. Gypsum appeared in some isolated

samples of this unit, sometimes reaching 10% of the mineral content.

Interval B (8.7–6.4 m) was marked by a progressive decrease in the quartz content, reaching its minimum value at 7.02 m (3.6%). Calcite was the dominant mineral and dolomite was scarce or absent. Silicate-group minerals (mostly muscovite) were also abundant.

Interval C (6.4–3.2 m) showed a clear augmentation of the quartz content (50–60%). Calcite+aragonite were not abundant (usually >10%) and dolomite content was generally below 5%. The mica-group and other silicate minerals were abundant, in some cases accounting for 40% of the total mineral fraction.

Magnetic susceptibility

The MS log revealed low values ($<15 \times 10^{-6}$ SI) in the E3 record (Figure 3), with some exceptions. The MS values in the lower part of the Holocene record (11.1–6.4 m) were very low ($< 2 \times 10^{-6}$ SI), with some interbeds with higher values (3–10 or 10–15 $\times 10^{-6}$ SI). The uppermost part of the record (>6.4 m) showed higher values ($>10 \times 10^{-6}$ SI), with some beds (5.5, 3.9, 3.8 m) $> 50 \times 10^{-6}$ SI.

Paleontology

Mollusks. A total of 82 mollusk genera were identified: 26 belonging to pelecipoda, 54 to gastropoda, 1 cephalopod, and 1 scaphopod (Table 1). Almost all pelecypoda corresponded to infaunal representatives, although there was a subtle presence of genera that preferred hard substrates (*Arca*, *Barbatia*, *Mytilus*, *Spondylus*, *Ostrea*). The gastropod Bivonia triquetra, typical of hard grounds, was also present. Thirteen genera were included in the micro-mollusk group (<10 mm in length). Of note, some macro-mollusks were represented by juvenile/very juvenile individuals when matching their size with micro-mollusk criteria, although they were not considered in that group. All species can be considered as common/very common in the Mediterranean Sea and are currently present in the area and mostly associated with *Posidonia* meadows (Belgacem et al., 2013).

To allow comparisons of the frequencies of individuals of each genera, we normalized the amounts to 100 g. This approach may lead to an artificial overrepresentation of uncommon genera.

Small pelecypoda shells of micro-mollusks and macro-mollusks at juvenile/very juvenile stages were well preserved, although large shells were broken. These shells showed net breaking lines and sharp edges, which can be interpreted as the result of crab predation (Belgacem et al., 2013; Hadlock, 1980; Lin, 1990; Torres et al., 2020; Walne and Dean, 1972). Gastropod shells were usually the most well preserved mollusks, in some cases, traces of bio-erosion, and breaking also occurred.

Figure 3 shows the total number of mollusks along core E3 and the total number of macro-mollusk shells after excluding those corresponding to the dominant micro-mollusks (*Bivonia triquetra*, *Granulina* sp., *Potamides conicus*, and *Rissoa* sp.). It is possible to observe the high contribution of

these genera, which doubled or even trebled the frequency of other mollusks.

Table 1. Mollusk genera present in the Holocene record of core E3.

Gastropoda	*Alvania*		*Potamides*
	Astraea		*Retusa*
	Bivonia		*Rhizorus*
	Bolma		*Rissoa*
	Bulla		*Rissoina*
	Caecus		*Scaphander*
	Caplyptraea		*Skenoidae*
	Cancellaria		*Smaragda*
	Cerithiopsis		*Tornus*
	Cythara		*Trophonopsis*
	Clanculus		*Truncatella*
	Coecus		*Turbonilla*
	Coelostraca		*Turtonia*
	Columbella	Pelecypoda	*Abra*
	Conus		*Anomia*
	Cyclichna		*Arca*
	Cyclope		*Barbatia*
	Cymatium ?		*Cardium*
	Dylvinella		*Cerastoderma*
	Eulimus		*Corbula*
	Epitonium		*Dosinia*
	Facsiolaria		*Gastrana*
	Fissurella		*Donacilla*
	Fusinus (Fusarius)		*Hiatella*
	Gibbula		*Irus irus*
	Gibberula		*Leptonia*
	Granulina		*Lima*
	Hadriania		*Loripes*
	Homalogyrus		*Mactra*
	Hydrobia		*Mytilus*
	Hynia		*Mytilaster*
	Jujubinus		*Nucula*
	Kelia		*Ostrea*
	Littorina		*Parvicardium*
	Mathilda		*Ruditapes*
	Melaniella		*Scrobicularia*
	Monodonta		*Spondylus*
	Ocinebrina		*Tellina*
	Paludinella		*Veneroidea*
	Patella	Cephalopoda	*Spirulina*
	Pisania	Scaphopoda	*Dentalium*

It must be highlighted that there was a high abundance of mollusks in the 9.6–9.0 and 8.7–6.4 m intervals, with macro-mollusks accounting for almost a third of the total. Moreover, at 4.8 m, there was an overwhelming presence of micro-mollusks and a residual presence of macro-mollusks. In contrast, in other intervals, the abundance of mollusks decreased, as did the diversity of species (11.1–9.6, 9.0–

8.7, and 6.4–3.1 m).

It is worth noting the presence of *Parvicardium exiguum* and *Cerastoderma glaucum* representatives showed an opposite pat- tern of occurrence, as the former appeared in 9.6–9.0 and 9.0–6.8 m intervals whereas the latter was absent (Figure 4). In contrast, *C. glaucum* shells were observed between 6.6 and 3.3 m, taking over from the presence of *P. exiguum*. It is remarkable that *Granulina*, *Bivonia triquetra* and *Rissoa* showed the same trend as *P. exiguum* (Figure 4), although the latter two genera were also present in the upper 6.4 m but were markedly less abundant than between 8.7 and 6.4 m.

Other mollusks, such as the minute turriculate gastropod *Potamides conicus*, appeared in high numbers in the whole E3 record, either within the euhaline association or in the brackish one (Figure 4). *P. conicus* is a detritivorous micro-gastropod. In many environments it forms clusters of hundreds of individuals, which colonize soft bottoms (Culha et al., 2018), as well as inter- tidal/subtidal environments of highly saline seas (Gützer, 2011; Zuschin and Gützer, 2014) and even continental saline environments (Kowalke, 2006).

Ostracoda. We identified 14 ostracoda genera within the Holocene record of core E3, although ostracoda shells were absent in the 11.1–9.6 and 9.0–8.7 m intervals (Figure 4). Two main asso- ciations were observed. The 9.6–9.0 and 8.7–6.4 m intervals showed high ostracoda abundance and species diversity: *Xestole- beris rubens* was predominant, followed by *Loxoconcha rhom- boidea*, *Loxoconcha elliptica*. *Propontocypris* sp. and *Neonesidea corpulenta*. *Cytheretta* sp., *Pontocythere* sp., *Carinocythereis whitei*, and *Cyprideis torosa* were present in few horizons. In con- trast, *C. torosa* was the only species present at >6.4 m.

Foraminifera. The diversity and abundance of foraminifera spe- cies varied along the Holocene record of core E3. To examine these parameters, we calculated the indexes shown in Figure 4. Foraminifera species were present in diverse intervals in the Holocene record. The following species were present between

11.1 and 10.0 m: *Ammonia beccarii, Elphidium crispum, Trilocu- lina trigonula, Elphidium macellum, Elphidium advenum, Nonion commune, Adelosina colomi, Quinqueloculina seminula, Quique- loculina duthiersi*, and *Quinqueloculina aglutinans*. However, there was a low diversity of species compared with other intervals, as revealed by the lowest values of the Shannon-Weaver (ca. 1), Equitability (0.5), and Fisher's alpha (<2) indexes (Figure 4).

At 10.0–9.6 m, *Q. duthiersi, Elphidium excavatum, E. crispum, A. beccarii, E. macelllum, Rosalina globularis*, and *Adelosina laevigata* occurred but they were poorly preserved. The diversity indexes in this interval showed a moderate increase, although the density of carapaces was still low (<100 n/g) (Figure 4).

The 9.6–9.0, and 8.7–6.4 m intervals showed a huge number of tests and species, including the following: *A. colomi, Elphidum aculeatum, E. crispum, Q. reticulata, Q. aglutinans, Triloculina trigonula, Sigmoilina grata, A. laevigata, Planorbulina mediter- ranea, Planorbulina variabilis, Rosalina mediterranensis, R. globularis, Peneroplis pertusus, E. advenum, Asterigerinata mamilla, Quinqueloculina bicornis, A. colomi, Miliolinella circu- laris, Masilina secans, E. excavatum, Miliolinella eburnea, E. advenum, Spiroloculina excavata, Lobatula lobatula*, and *Q. sem- inula*. Indeed, these intervals showed the highest values of all the indexes (Figure 4).

In contrast, in the 9.0–8.7 m interval and in the uppermost 6.4 m, forams were scarce and those present were poorly preserved. In this regard, there was a very low density of foraminifera tests, although the

Equitability index indicated that the number of species and individuals of each one were balanced. The Shannon- Weaver index pointed to an impoverished ecosystem.

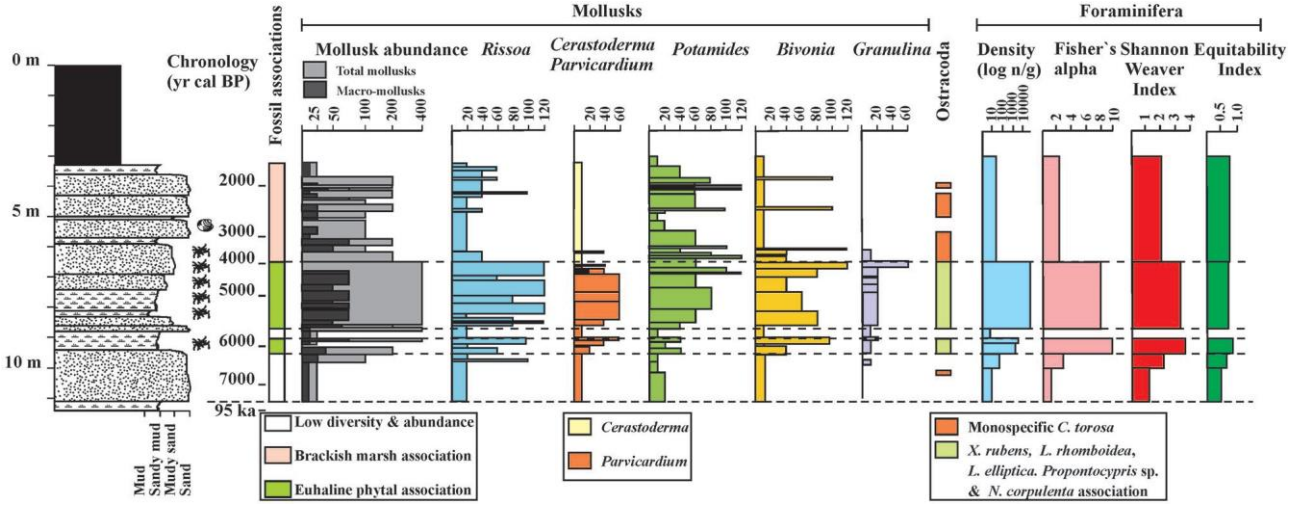

Figure 4. Downcore plots of total mollusk content, abundance of *Bivonia, Cerastoderma, Parvicardium, Rissoa, Granulina* and *Potamides* representatives, ostracoda associations, and the Density index, Shannon-Weaver index, Fisher's alpha index, and Equitability index of foraminifera, together with the environmental interpretation.

Paleobotany. From the bottom of the Holocene record to 6.7 m, there was a continuous presence of plant (genus indet) seeds and a noticeable lack of *Chara* oogonia, which appeared in the Holocene age deposits of the nearby El Almarjal marsh (Torres et al., 2018).

Of note, tangles of decayed leaves belonging to *Posidonia oceanica* and *Cymodocea nodosa* appeared, being abundant at 9.5–9.0, 8.2–8.0, and 7.8–6.8 m and having a moderate presence at 6.8–6.2 m (Figure 4).

The seagrasses *P. oceanica* and *C. nodosa* are typical in shal- low Mediterranean Sea bottoms. Generally, the former forms the most common, productive and widespread meadows of this water body and represents the marine system with the highest levels of biodiversity (Gallmetzer et al., 2005; Gobert et al., 2006; Lepoint et al., 2006; Mazzella et al., 1993; Tomasello et al., 2018).

Discussion

The morphology of the Holocene Basin

According to the chronological model obtained from ^{14}C and AAR ages, the Holocene record began in the E3 area at ca. 7300 yr cal BP. There was no record of earlier Holocene because of the sea-level position. Thus, this date implies a certain delay in the start of the Holocene transgression when compared with the ages proposed by Vacchi et al. (2016, 2018) and Rovere et al. (2016). However, Vacchi et al. (2018) found small differences between five coastal basins in the western Mediterranean realm. In this regard, the geophysical research revealed that Holocene sedimentation began with ancient paleo-channel infills, which may con- tain an almost complete marine record of the Holocene.

It should be noted that the Holocene transgression did not take place on a lineal coastal morphology

but on a pre-existing flat valley or coastal plain formed during MIS5 times (Torres et al., 2018). From MIS5 to MIS2, the valley was under erosive conditions (Torres et al., 2018). Indeed, the age of the Pleisto- cene record in core E3 at 11.5 m was ca. 95 ka (Ortiz et al., 2021; Torres et al., 2019), meaning that the youngest sub-episodes of MIS5 and MIS4-2 were not deposited or that those materials were eroded, the debris being transported to the sea along the erosive channels that the marine geophysics revealed (Figure 2). We can tentatively postulate that these erosive morphologies channeled the seawater flow of the Holocene transgression as they were filled by the oldest Holocene deposits which were well-stratified (Torres et al., 2018).

These processes of basin (river mouth, paleo-valleys) infill controlled by pre-existing geoforms have been interpreted in other places, including the mouth of the river Tagus (Vis et al., 2008, 2010), the Rhine estuary (Hijma et al., 2009), the Po delta (Rossi and Vaiani, 2008), Brittany (Menier et al., 2010), the Elbe river (Hepp et al., 2019), and the Languedocian lagoons (Raynal et al., 2010).

In the Cartagena area, there was clear geophysical evidence that the former paleovalley river (Benipila Creek) was drowned (Bailey et al., 2020), but the Holocene transgression was also responsible for changes on the mainland. These changes were linked to the sudden and rapid change of the base level landwards, affecting the phreatic level. In this regard, the development of an extensive saline marsh in El Almarjal can be explained by the rise of the phreatic level, with short marine ingressions being common (Torres et al., 2018).

Thus, the Early Holocene (Greenlandian, Walker et al., 2012, 2018) was not registered in the Cartagena coastal record, nor was the beginning of the Middle Holocene (Norgrippian). In contrast, the Late-Holocene (Meghalayan) was fully recorded.

Environmental evolution

For the interpretation of the paleoenvironmental conditions, we firstly considered the MS and also Si and Br normalized to Al (Figure 3), these latter parameters presented in Ortiz et al. (2021), as they are the most common element ratios used as proxies for fluvial terrigenous inputs and reducing environments, respectively (Frigola et al., 2007; Martinez-Ruiz et al., 2015; Martín- Puertas et al., 2010; Nieto-Moreno et al., 2011, 2013).

MS may indicate the input of detrital sediments into the basin. However, MS did not show any correspondence with the sediment characteristics of the E3 record, as sand beds provided either high or low MS values. It should be noted that reductive iron oxide dissolution commonly occurs in organic-rich sediments, where reducing conditions linked to the presence of organic matter result in the dissolution of magnetic particles (Canfield and Berner, 1987; Dekkers, 1997; Murdock et al., 2013; Nowaczyk et al., 2004; Ortega et al., 2006). Here, the organic content (C_{org}) was inversely related to the paramagnetic mineral content and may indicate reductive iron oxide dissolution processes when C_{org} increased. Thus, it appears that in samples from the E3 core MS was regulated mainly by a low input of iron minerals and organic matter content.

It is worth noting that in the lower part of the profile (11.1– 9.6 m), coinciding with a sandy bed, both MS and C_{org} showed low values. Furthermore, the fossil content was very scarce or even absent. However, the Si/Al ratio showed the highest values, indicating fluvial input (Martín-Puertas et al., 2010; Nieto- Moreno et al., 2011, 2013; Ortiz et al., 2021), probably related to the fan delta that developed at the mouth of the Benipila Creek (Torres et al., 2018). In this regard, quartz predominated, and there was a significant presence of calcite and dolomite. Given that these minerals are diamagnetic, their presence should have decreased the MS values.

Fossil associations. The fossil assemblages allowed us to define two environments, namely euhaline phytal and brackish (Figure 4).

The euhaline phytal association was characterized by a rich biodiversity of mollusks (Table 1), ostracoda and foraminifera (Figure 4), together with *Posidonia* and *Cymodocea* tangles, which occurred at 9.6–9.0 and 8.7–6.4 m intervals.

The most characteristic feature of this association was the presence of the mollusks *P. exiguum* and *Granulina* (which were absent in other intervals), together with a high abundance of *Bivonia triquetra* and *Rissoa*. Furthermore, *X. rubens*, *L. elliptica*, *L. rhomboidea*, all linked to phytal environments, were found only within this association.

P. exiguum is a small cardiodea that usually appears in associa- tion with seagrass meadows (Uzunova, 2010). The micro-gastro- pod *Granulina* (*Marginella*) is a common inhabitant of *Posidonia* meadows (Antit et al., 2013; Urra et al., 2013). *Rissoa* is also a minute gastropod that, in the Mediterranean realm, includes many species, and colonizes soft bottoms covered by seagrass, where it grazes on algae and bacteria (Gofas et al., 2011). *B. triquetra*, a sessile organism that inhabits the intertidal zone (Sisma-Ventura et al., 2020). Although very little is known about the development phases of *B. triquetra*, Calvo and Templado (2005) defined swimming/crawling behavior during the pediveliger stage. This feature is not irrelevant in the E3 record because we found hundreds of free individuals.

The main ostracoda species of this association was *X. rubens*, followed by *L. rhomboidea*, *L. elliptica*. *Propontocypris* sp., and *N. corpulenta*, with *Cytheretta* sp., *Pontocythere* sp., and *C. whitei* present in few horizons. In coherence with the consider- ations made through the mollusk association, the high frequencies of *X. rubens* (>40%) were interpreted as greater abundance and/ or density of sub-aquatic vegetation (Athersuch, 1979; Cronin et al., 2001), as it is a typical phytal indicator of euryhaline shallow-water vegetate bottoms like those belonging to the biocenosis of the *Posidonia* meadow (Triantaphyllou et al., 2010). *Loxocon- cha* spp is a survivor-type ostracoda that tolerates fluctuating salinity (Lachenal, 1989; Stone et al., 2000) and hypoxic waters (Alvarez Zarikian et al., 2000; Bodergat et al., 1997, 1998). The presence of *L. rhomboidea* may indicate more open environments with a greater influence of marine water (Ruiz et al., 2000a; Smith and Horne, 2002), and it is considered a typical phytal species (Althersuch et al., 1989). Moreover, representatives of *Proponto- cypris* spp are more common on sublittoral phytal and coralline substrates (Maddocks,

1966, 1969). Similarly, *N. corpulenta* is considered a nearshore species limited to shallow marine environments, rich in bottom vegetation (Bonaduce et al., 1976; Mad- docks, 1969; Sciuto et al., 2015; Szczechura, 2006). Likewise, *Cytheretta* sp., *Pontocythere* sp. and *C. whitei* are typical coastal infralittoral euryhaline (30–40‰) ostracoda (Nachite et al., 2010; Ruiz et al., 2000a, 2000b, 2003), characteristic of coastal phytal and periphytal environments (Ruiz et al., 2000a).

Coinciding with the information provided by mollusks and ostracoda, foraminifera showed a high abundance and diversity of species, as reflected by the indexes calculated. Thus, this association is considered a marker of euhaline conditions (marine) with soft bottoms covered by *Posidonia* and *Cymodocea* meadows, which produce high biodiversity.

The brackish marsh association, which occurred between 6.4 and 3.1 m, was characterized by a decrease in both the abundance and diversity of mollusk species (Figure 4). It was marked by the presence of *C. glaucum* (absent below 6.4 m), which has wide tolerance to fluctuations in salinity, although it is a flourishing colonizer of brackish water masses (Anadón, 1989; Rich- ards, 1985; Torres et al., 2018). Here, C. glaucum representatives corresponded, in most cases, to juveniles, thereby indicating environmental stress caused by low salinity or emersion. It is worth noting that *C. glaucum* is a well-known inhabitant of the Holocene sediments in the marshy area of El Almarjal (Torres et al., 2018).

Other less frequent species were *Hydrobia* sp., which is also typical of a brackish water environment (Brown et al., 1975; Saxena, 2005), and *Loripes lacteus*, typical of anoxic sulfur-rich muddy bottoms (Rossi et al., 2013). Other taxa also present in this association were *Bivonia*, *Rissoa* and *Potamides*, showing a marked decrease in abundance with respect to the euhaline association.

It is worth noting that *Cyprideis torosa* was the only ostracoda species present, except for three horizons in which *Heterocypris salina* also occurred. *C. torosa* can inhabit waters with a wide range of salinity, varying from freshwater to hyperhaline (0.5– 60‰) (De Deckker, 1981), and can be found together with a vari- ety of ostracoda species. However, coastal lagoons have ostracoda assemblages with very low diversities, characterized by brackish taxa accompanying *C. torosa*, which is frequently predominant (Pint and Frenzel, 2017). Monospecific occurrences of *C. torosa* occur mainly in hypersaline environments, but also in lagoonal brackish environments.

This fossil association was also characterized by low species richness and specimen abundance for foraminifera. Foraminifera tests revealed the presence of *Ammonia beccarii* while other planktonic representatives were virtually absent.

These species associations, therefore, indicated an oligohaline or low mesohaline shallow-water environment, probably in a pro- tected water mass with sporadic marine influence.

Paleoenvironmental units. According to the interpretation of the sedimentological, mineralogical, paleontological, and geochemi- cal proxies, there were changes in the paleoenvironmental conditions in the area. We were able to establish three units: coastal conditions influenced by fluvial inputs (Unit A), open marine conditions at 9.6–6.4 m (Unit B), and restricted brackish marsh at 6.4–3.1 m (Unit C).

Unit A (11.1–9.6 m; 7300–6300 yr cal BP). This unit was characterized by a sandy bed, which consisted of medium-size grains made of quartz, calcite, and dolomite grains, producing low MS. The fossil content was scarce, except for the uppermost part, in which some marine mollusks appeared, although the diversity and abundance of foraminifera were very low. We pro- pose that the shifts toward very low quartz percentages observed at 9.7 and 9.4 m are explained by the abundance of bioclastic material in the sample.

We interpreted that these materials were deposited in a shallow marine environment (beach?) with a strong fluvial influence of the Benipila Creek delta (Figure 5a), as indicated by high Si/Al values accompanied by low C_{org}. This activity was probably linked to the "mise en place" of the Benipila Creek fan delta.

Unit B (9.6–6.4 m; 6300–3800 yr cal BP). This unit was characterized by low MS and Si/Al values, high Br/Al and C_{org} values, abundant *Posidonia* phytoclasts, and it was colonized by the euryhaline association of fauna typical of phytal environments.

Thus, there was a stable shallow marine environment with the development of a *P. oceanica* meadow that served as a nursery, shelter, and grazing area for a high diversity of mollusk and ostracoda species, and where filtering organisms, such as foraminifera, thrived (Figure 5b).

The presence of *Posidonia* beds marked the marine limiting line, which can be interpreted as an inner bay environment (McGlathery et al., 2007) with growing eutrophication processes. The presence of gray to dark muds, silty muds and fine sands, rich in calcite, together with high values of C_{org} and Br/Al and low values of Si/Al, indicated low detrital input and organic matter preservation under low energy conditions. Thus, relative anoxic bottoms were likely to occur. Further- more, low values of MS may indicate the input of detrital sediments into the basin and/or reductive iron oxide dissolution processes when C_{org} increased (Canfield and Berner, 1987; Dekkers, 1997; Murdock et al., 2013; Nowaczyk et al., 2004; Ortega et al., 2006). Likewise, according to Ziegler et al. (2008), bromine in sediments are exclusively linked to marine environments.

Mollusks, ostracoda, and foraminifera showed a high biodi- versity of species, which points to euhaline conditions (marine) with an abundance of typical phytal indicators of shallow-water vegetate bottoms.

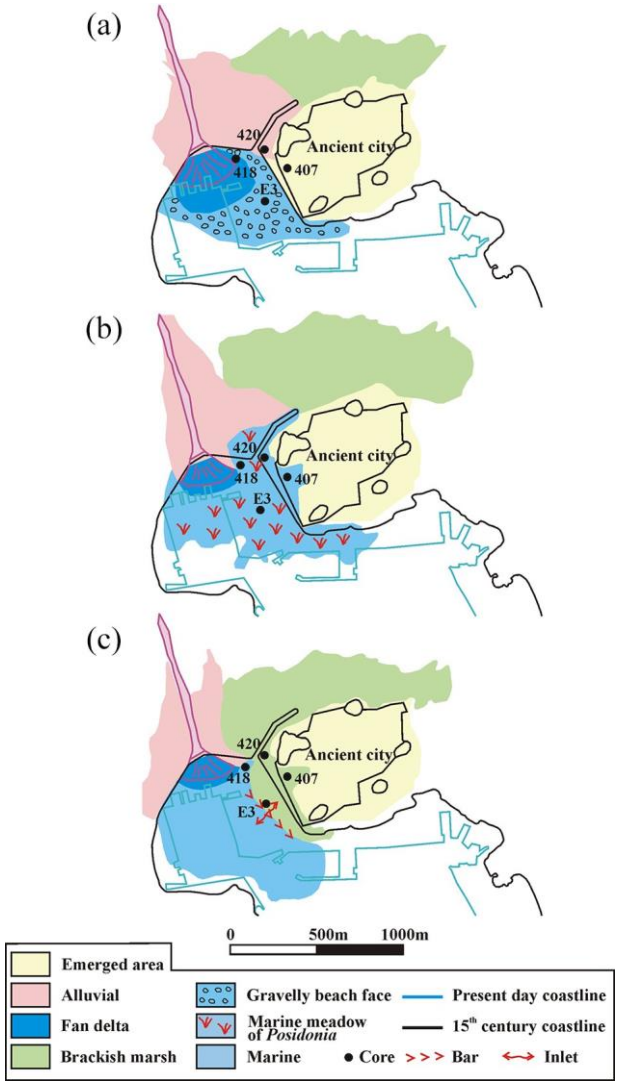

Figure 5. Paleogeographical scenarios in Cartagena with the facies distribution: (a) during Unit A (7300–6300 yr cal BP); (b) during Unit B (9.6–6.4 m; 6300–3800 yr cal BP); and (c) during Unit C (3800– 1600 yr cal BP). For reference of the location map, see Figure 1.

It must be highlighted that between 9.0 and 8.7 m (5850– 5650 yr cal BP), there was a short pulse of the alluvial fan input into the marine realm, as attested by the increase of Si/Al values. Moreover, from the paleobiological perspective, this episode was devoid of macro-mollusks and ostracoda, and foraminifera were scarce. Only micro-mollusks (*Rissoa, Bivonia, Potamides, Gran- ulina*) appeared, but in low frequencies (transported?).

Toward the top of Unit B, a certain degradation of the ecosystem was detected as *Posidonia* remains, foraminifera, *Parvicardium*, and *Rissoa* (temporally) vanished. The MS values and Si/Al ratio indicated that silting began at this time, although marine species still survived at low frequencies. *C. glaucum* presence was also detected.

Unit C (6. 4–3.1 m; 3800–1600 yr cal BP). In contrast to the previous unit, in Unit C, sandy beds occurred, showing an increase in quartz content, the mica-group and other silicate minerals being abundant, thereby indicating more detrital input. Indeed, the MS values and Si/Al ratio increased, whereas the Br/Al ratio and C_{org} significantly decreased. It is remarkable that *Posidonia* remains

disappeared, and euhaline fauna (*P. exiguum*, *B. trique- tra*, *Rissoa* spp.) was substituted by the brackish water association (characterized by the presence of *C. glaucum* and *C. torosa*), with less diversity of macro-mollusk and ostracoda, and foraminifera almost totally disappeared. The most abundant micro mollusk was *P. conicus*, an ever-present inhabitant of marine and marsh environments in the area (Torres et al., 2019, 2020).

Thus, we interpreted that this unit occurred in a marsh partially isolated from the sea by a chenier-like barrier made of shells and *Posidonia* fragments, possibly with small passageways that communicated the sea and dry land (Figure 5c).

Influence of anthropic activities

Special attention was paid to complete the paleoenvironmental reconstruction of Cartagena during the last ca. 2300 yr (top of Unit C), a period characterized by the rise of the city and an important occupation that markedly disturbed sea bottoms and sedimentary sequences (Torres et al., 2018). To this end, we also studied the uppermost part of sequence E1, located close to core E3. We chose this section (E1) as, in spite of a strong anthropic influence during this period, the E1 record remained almost undisturbed, although with human influence. The anthropic influence was previously interpreted in this area through the presence of metal-polluted beds attesting metallurgical activity (Ortiz et al., 2021, 2022), formerly detected in cores from El Almarjal marsh (Manteca et al., 2017). In the present study, we focused on the sedimentological characteristics.

The interrelation of changes in geoforms and anthropic activity has been widely discussed in other areas (Anthony et al., 2014; Marriner and Morhange, 2007; Marriner et al., 2006, 2014; Morhange et al., 2000). However, in our case, the interpretation was constrained by the reduced observation offered by the E1 section. In this regard, the lowermost 3.7 m of the E1 sequence (black muds with drifted *P. oceanica* remains and articulated *Pinna nobilis*, followed by fine sands with pelecipoda shells) can be cor- related with core E3 (Figure 6): units B and C were clearly identifiable in E1, although a hiatus may occurred at 6.2–5.6 m, between ca. 5500 and 3000 yr cal BP (Torres et al., 2018), which could be linked to port work (dredging) undertaken to gain depth in a muddy coastal approach. However, some differences attributable to anthropic influence were observed between the 4.2 and 2.6 m of the E1 sequence and characteristics of E3 (Unit C). Indeed, the 3.9–4.2 m (E1) interval consisted of flat oriented pottery sherds in a sandy bed. Many stakes made of slender pine logs were driven into the underlying Unit C. Three ^{14}C ages (Table 2) placed these stakes in the Punic period. These findings may indicate the use of these stakes to drag or condition a sea-dryland "channel" in order to overcome the barrier ("chenier") that protected a muddy shallow brackish marsh. Thus, we interpreted that the E1 hiatus was the result of dredging the muddy bottom.

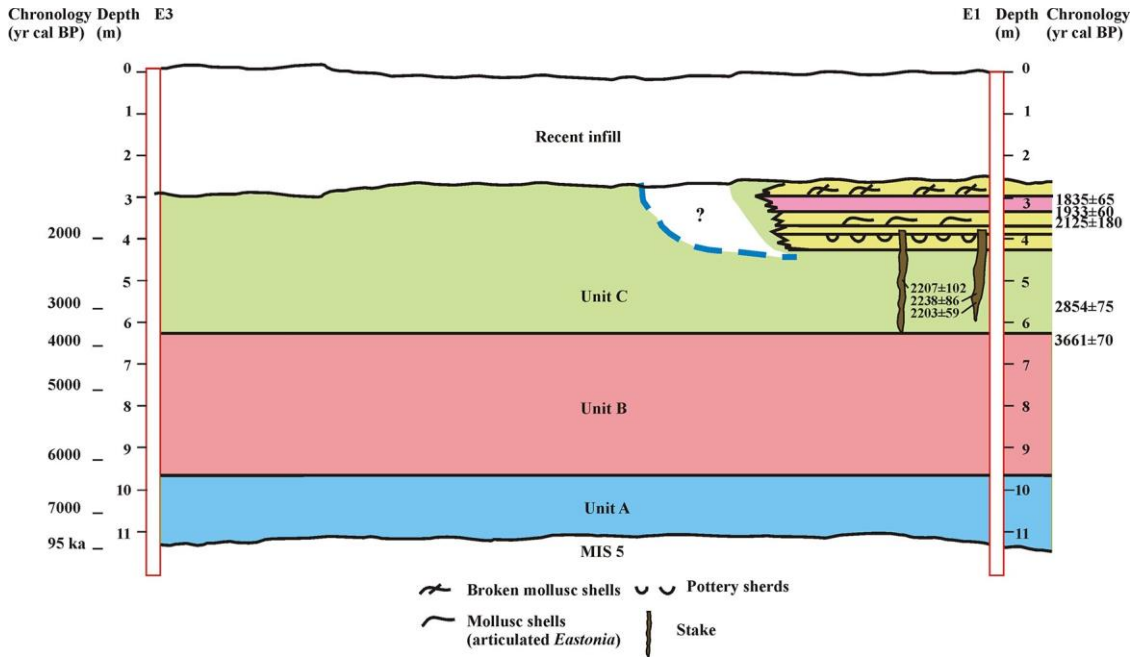

Figure 6. Correlation between core E3 and E1 sequences. Units A, B, and C are identified.

Table 2. Radiocarbon age (yr BP) of selected levels from E1 sequence and calibrated age (yr cal) converted using the Radiocarbon Calibration Program 8.2 (CALIB 8.2) (Stuiver et al., 2021) with the calibration dataset IntCal20 (Reimer et al., 2020) for the wood, plant, and charred material, and the MARINE20 calibration curve (Heaton et al., 2020) for the marine shell.

Sample no.	Material	Depth (m)	$\delta^{13}C$ (V-PDB)	Conventional age BP	Calibrated BP
Beta-490660	Wood	Stake	−26.3	2170 ± 30	2052–2308
Beta-490661	Wood	Stake	−29.3	2220 ± 30	2146–2333
Beta-464997	Wood	Stake	−24.6	2240 ± 30	2151–2338
Beta-464998	Plant	2.9	−26.0	1980 ± 30	1863–1991
Beta-464999	Plant	5.6	−10.1	2760 ± 30	2776–2937
Beta-465000	Plant	6.3	−12.5	3430 ± 30	3575–3726
Beta-465332	Charred material	2.9	−21.9	1900 ± 30	1728–1887
CNA-5841	*E. rugosa* shell	3.5	1.7	2436 ± 30	1945–2305

The forced development of coastal conditions, as saline waters entered the area, led to the sedimentation of pale yellow fine sands with large articulated clam valves between 3.8 and 3.3 m (Figure 6). Only representatives of a thermophile tropical-affinity species (*Eastonia rugosa*) (Soriano et al., 2010) were observed in this interval dated at 2125 ± 180 yr cal BP, indicating that warm conditions occurred during the Roman period (in Torres et al. 2018) they were erroneously attributed to *R. decussatus*). This bed was followed by dark brown massive clay (3.3–2.9 m) linked to sediment input from dry land as a result of a flood period, and yellowish sands with pelecypoda shells, including *Rissoa* and *Bivonia* (2.9–2.8 m), indicating the reactivation of marked marine influence. A thin black bed comprising charred vegetal remains occurred at its top, dated at 1935 ± 60 yr cal BP and 1835 ± 65 yr cal BP. Scattered well-rounded gravel also appeared. The sequence ended with pale yellow fine sands with medium-scale cross bedding (2.8–2.6 m).

Thus, from 2300 to 1600 yr cal BP, Cartagena provided safe anchorage and port facilities for Punic and Roman ships. It seemed that the first inlet amenagement took place during Punic times as reflected

by ^{14}C ages from the stakes driven into the sea bottom and a pottery sherd accumulation took place. Later during Roman times the inlet was still active as a bidirectional duct channeling runoff from the nearby hills as attested by a thick bed of red mud of alluvial origin. During Roman period under short- timed the marine influence a rapid sand infill deactivated its functional use. In any case dragging works, that probably took place in any measure, were quite different of other of the Mediterranean realm (Carsana et al., 2009) although the limited exposure does not allow to obtain more conclusive information.

Later, to favor naval operations, intense dredging activities and moles (wave breakers) distorted the pristine aspect of Cartagena Bay. In the open marine realm of Cartagena Bay, dredging processes, probably since the XV century, removed the uppermost part of the Holocene record, as attested by evidence provided by marine geophysics.

The characteristics of the E1 sequence reinforces the observations made by Melis et al. (2018), who noted that coastal modifications during the Holocene were driven by the interplay of climate, geomorphological processes and human activity. In Cartagena, which has been the most important safe port in the Spanish Mediterranean coast since at least Phoenician times, a series of works were done to improve land and port access. The uppermost part of the E1 record reflected a limited attempt to achieve this access, but the effect of torrential flooding, typical of the Mediterranean climate, thwarted these efforts and the record resulted biased (Marriner et al., 2006), as suggested by the presence of pale yellow sands. Giaime et al. (2019) described the development of ancient harbors in deltaic contexts and, in fact, a small-scale fan-delta regime dominated in Cartagena Bay. Channel digging probably altered the ecological equilib- rium of the uppermost part of the Unit C record slightly, as sug- gested by Morhange et al. (2016). An ancient map of the 17th century (Figure 7) drawn after a severe flood that affected the navy base, before the development of the modern city, reveals an inlet (a creek mouth) across the marsh being a good analog of the upper part of the E1 record.

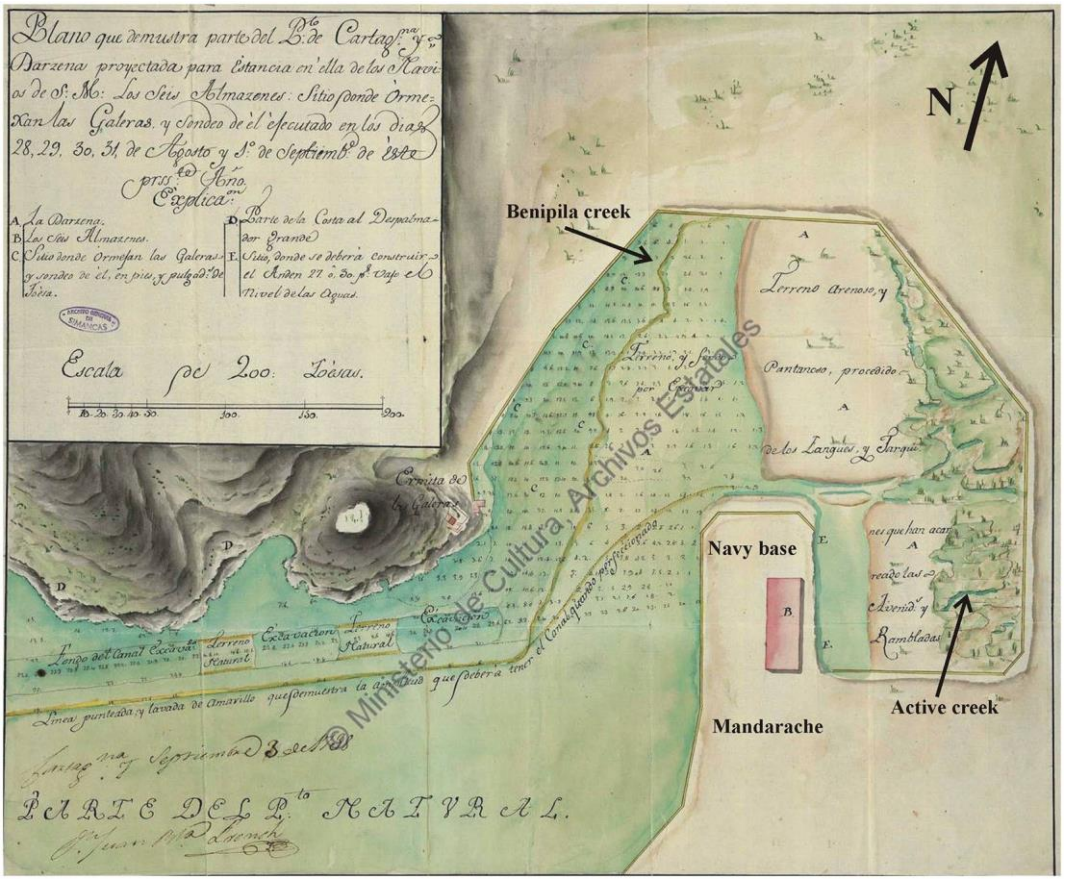

Figure 7. Anonymous 1738 map of the Cartagena Bay, including the Navy Base area, showing the silted zone after a highly severe flash flood.

Conclusions

The Holocene evolution of the Cartagena basin was obtained through a detailed multidisciplinary study of a new core named E3. The Holocene record began at ca. 7300 yr cal BP, filling the pre-existing valley, excavated on a coastal plain of, at least, MIS5c age.

The Holocene transgression deeply affected the area: a series of fan-deltas developed, as reflected by the detrital inputs in the E1 and E3 records. The new position of the base level led to the development of a very shallow phreatic level, which caused waterlogging of the "El Almarjal" area, where episodic marine ingressions occurred. This process was reflected in a rapid silting- up of the area, as confirmed by geochemical data, in such a way that full marine conditions occurred from 7300 to 3800 yr cal BP, as reflected by mollusk and foraminifera biodiversity, which changed to a biologically impoverished brackish marshy-environment between 3800 and 1600 yr cal BP linked to the development of a sandy-muddy bar (chenier).

The marked differences between the top of the E1 and E3 sequences allowed us to deduce the presence of a micro-land- scape because of anthropic influence during Punic and Roman times. E3 reflected a homogeneous flat marsh while in E1 a pre- existing erosive inlet was altered by humans to give access to dry land, as attested by pottery sherds and by logs of Punic age, which were driven into the underlying sediments. This wooden structure favored a certain degree of marine influence on the surrounding area, as reflected in the E3 record, but this influence was short- lived because the zone was quickly filled by sand.

Thus, this environment of the area changed from an open marine to a marsh environment, probably caused by intense silting linked to processes that allowed the buildup of a bar that partially isolated a narrow strip of the marsh from the sea.

Acknowledgements

We thank Prof. Pedro JM Costa and an anonymous reviewer for their helpful comments.

Funding

The author(s) disclosed receipt of the following financial support for the research, authorship, and/or publication of this article: This paper was made possible by Grant HAR2017-85726-C2-2-P (*Cambios ambientales y ocupación humana en el sector central del sureste ibérico*) funded by MCIN/AEI/ 10.13039/501100011033 and by Grant HAR2017-85726-C2-1-P (*Carthago Nova desde su entorno litoral: Paleotopografía y evolución medioambiental del Sector central del Sureste Ibérico. Dinámica poblacional y pro- ductiva*) funded by MCIN/AEI/ 10.13039/501100011033.

ORCID iDs

José E Ortiz https://orcid.org/0000-0002-5699-2593 Sebastián Ramallohttps://orcid.org/0000-0003-1828-3996

References

Althersuch J, Horne DJ and Whittaker JE (1989) Marine and brackish water ostracods (Superfamilies Cypridacea and Cytheracea). In: Kermack DM and Barnes RSK (eds) *Synopses of the British Fauna, New Series, 43*. Leiden: EJ Brill, 343pp

Alvarez Zarikian CA, Blackwelder PL, Hood T et al. (2000) Ostra- cods as indicators of natural and anthropogenically-induced changes in coastal marine environments. Coasts at the Millennium. In: *Proceedings of the 17th international conference of the coastal society*, Portland, 9–12 July, pp.896–905.

Anadón P (1989) Los lagos salinos interiores (atalásicos) con faunas de afinidad marina del Cenozoico de la Península Ibérica. *Acta Geologica Hispanica* 24: 83–102.

Anthony EJ, Marriner N and Morhange C (2014) Human influence and the changing geomorphology of Mediterranean del- tas and coasts over the last 6000years: From progradation to destruction phase? *Earth-Science Reviews* 139: 336–361.

Antit M, Daoulatli A, Rueda JL et al. (2013) Temporal variation of the algae-associated molluscan assemblage of artificial substrata in Bay of Tunis (Tunisia). *Mediterranean Marine Science* 14(2): 390–402.

Arduino G, Arduino M, Nappo A et al. (2016) *Conchiglie del Mediterraneo*. Available at: http://www.conchigliedelmedi- terraneo.it/ (accessed 10 July 2016).

Athersuch J (1979) The ecology and distribution of the littoral ostracods of Cyprus. *Journal of Natural History* 13: 135–160. Bailey G, Galanidou N, Peeters H et al. (2020) *The Archaeology of Europe's Drowned Landscapes*. Dordrecht: Springer Nature.

Begon M, Harper JL and Townsend CR (1996) *Ecology: Indi- viduals, Populations, and Communities*. Cambridge, MA: Blackwell Science Ltd.

Belgacem W, Langar H, Pergent G et al. (2013) Associated mol- lusc communities of a *Posidonia oceanica* meadow in Cap Zebib (off North East Tunisia). *Aquatic Botany* 104: 170–175. Benjamin J, Rovere A, Fontana A et al. (2017) Late quaternary sea-level changes and early human societies in the central and eastern Mediterranean Basin: An interdisciplinary review. *Quaternary International* 449: 29–57.

Blaauw M and Christen JA (2011) Flexible paleoclimate age- depth models using an autoregressive gamma process. *Bayes- ian Analysis* 6: 457–474.

Boar RR and Harper DM (2002) Magnetic susceptibilities of lake sediment and soils on the shoreline of Lake Naivasha, Kenya. In: Harper DM, Boar RR, Everard M et al. (eds) *Lake Naivasha, Kenya Developments in Hydrobiology*. Dordrecht: Springer, pp.81–88.

Bode M, Rothenhoefer P, Hanel N et al. (2015) Lead-silver mines of the Iberian Peninsula and their exploiters: A reconstruction of roman lead production in southeastern Spain. In: *Abstract book of the 4th Archaeometallurgy in Europe international conference*, Madrid, 1–3 June 2015, 80pp.

Bodergat AM, Jkceya N and Irzi Z (1998) Domestic and industrial pollution: Use of ostracods (Crustacea) as sentinels in the marine coastal environment. *Journal de Recherche Océanographique* 23: 139–144.

Bodergat AM, Rio M and Ikeya N (1997) Tide versus eutrophication. Impact on ostracods populations structure of Mikawa Bay (Japan). *Revue de Micropaleontologie* 40: 3–13.

Bonaduce G, Ciampo G and Masoli M (1976) Distribution of Ostracoda in the Adriatic Sea. *Pubblicazioni della Stazione Zoologica di Napoli* 40 Suppl: 1–304.

Bright J and Kaufman DS (2011) Amino acid racemization in lacustrine ostracodes, part I: Effect of oxidizing pre-treat- ments on amino acid composition. *Quaternary Geochronology* 6: 154–173.

Brown RC, Gilbertson DD, Green CP et al. (1975) Stratigraphy and environmental significance of Pleistocene deposits at Stone, Hampshire. *Proceedings of the Geologists Association* 86: 349–363.

Calvo M and Templado J (2005) Reproduction and development in a vermetid gastropod, *Vermetus triquetrus. Invertebrate Biology* 123: 289–303.

Canfield DE and Berner RA (1987) Dissolution and pyritization of magnetite in anoxie marine sediments. *Geochimica et Cosmochimica Acta* 51: 645–659.

Carbonel P (1985) Néogène. In: Oertli HJ (ed.) *Atlas des ostra- codes de France. Bulletin des Centres de Recherches Exploration-Production Elf-Aquitaine*, vol. 9. pp.311–335.

Carrión JS, Fierro E, Ros M et al. (2018) Ancient forests in European drylands: Holocene palaeoecological record of Maz- arrón, south-eastern Spain. *Proceedings of the Geologists Association* 129: 512–525.

Carsana V, Febbraro S, Giampaola D et al. (2009) Evoluzione del paesaggio costiero tra Parthenopee Neapolis. *Méditerranée* 112: 14–22.

Cerezo F (2016) *Los puertos antiguos de Cartagena: geoarqueología, arqueología portuaria y paisaje marítimo: un estudio desde la arqueología náutica*. PhD Thesis, Universidad de Murcia.

Chan LS, Yeung CH, Yim WWS et al. (1998) Correlation between magnetic susceptibility and distribution of heavy metals in contaminated sea-floor sediments of Hong Kong harbour. *Environmental Geology* 36(1–2): 77–86.

Conesa C and García-García E (2003) Las áreas históricas de inundación en Cartagena: problemas de drenaje y actuacio- nes. *BAGE: Boletín de la Asociación de Geógrafos Españoles* 35: 79–100.

Cronin TM, Holmes CW, Brewster-Wingard GL et al. (2001) Historical trends in epiphytal ostracodes from Florida Bay: Implications for seagrass and macro-benthic algal variability. *Bulletins of American Paleontology* 361: 199–231.

Culha M, Haksoy O and Tatarhan GE (2018) Soft bottom mollusk assemblages (gastropoda-Bivalbia) in marine shallow water of the western Turkey coast. *Indian Journal Geo Marine Sciences* 47: 2296–2304.

D'Angelo G and Gargiullo S (1978) *Guida alle conchiglie mediterranee: conoscerle, cercarle, collezionarle*. Kilano: Fabbri.

De Deckker P (1981) Ostracods of athalassic saline lakes. *Hydrobiologia* 81–82: 131–144.

Dekkers MJ (1997) Environmental magnetism: An introduction. *Geologie en Mijnbouw* 76: 163–182.

Domergue C (1990) Les mines de la Peninsule Ibérique dans l'Antiquité romaine. *Publications de l'École française de Rome* 127: 1–696.

Evans AM, Flatman JC and Flemming NC (2014) *Prehistoric Archaeology on the Continental Shelf: A Global Review*. New York, NY: Springer.

Fisher RA, Corbet AS and Williams CB (1943) The relation between the number of species and the number of individuals in a random sample of an animal population. *Journal of Ani- mal Ecology* 12: 42–58.

Flemming NC, Harff J, Moura D et al. (2017) *Submerged Landscapes of the European Continental Shelf: Quaternary Paleoenvironments*, vol. 1. Chichester: Wiley-Blackwell.

Frigola J, Moreno A, Cacho I et al. (2007) Holocene climate variability in the western Mediterranean region from a deepwater sediment record. *Paleoceanography* 22: 2209.

Gallmetzer I, Pflugfelder B, Zekely J et al. (2005) Macrofauna diversity in Posidonia oceanica detritus: Distribution and diversity of mobile macrofauna in shallow sublittoral accumulations of *Posidonia oceanica* detritus. *Marine Biology* 147: 517–523.

Ghilardi M, Kunesch S, Styllas M et al. (2008) Reconstruction of mid-Holocene sedimentary environments in the central part of the Thessaloniki Plain (Greece) based on microfaunal identification, magnetic susceptibility and grain-size analy- ses. *Geomorphology* 97: 617–630.

Giaime M, Marriner N and Morhange C (2019) Evolution of ancient harbours in deltaic contexts: A geoarchaeological typology. *Earth-Science Reviews* 191: 141–167.

Giannuzzi–Savelli R, Pusateri F, Palmeri A et al. (1997) *Atlante delle conchiglie marine del Mediterráneo, Vol. 2, Caenogas- tropoda parte 1*. Rome: Edizioni de "La Conchiglia".

Gobert S, Cambridge ML, Velimirov B et al. (2006) Biology of *Posidonia*. In: Larkum AWD, Orth RJ and Duarte CM (eds) *Seagrasses: Biology, Ecology, and Conservation*. Dordrecht: Springer, pp.387–408.

Gofas S, Salas C and Moreno D (2011) *Moluscos marinos de Andalucía (vol 1)*. Málaga: Servicio de Publicaciones e Inter- cambio Científico, Universidad de Málaga.

Guillaume MC, Peypouquet JP and Tetart J (1985) Quaternaire et Actuel. In: Oertli HJ (ed.) *Atlas des ostracodes de France. Bulletin des Centres de Recherches Exploration-Production Elf-Aquitaine*, vol. 9. pp.337–377.

Gützer CC (2011) *Habitat mapping and molluscan zonation of a Red Sea tidal flat at Dahab (Gulf of Aqaba, Egypt)*. PhD Thesis, University of Wien, Austria.

Hadlock RP (1980) Alarm response of the intertidalsnail Littorina littorea (L.) to predation by the Crabcarcinus maenas (L.). *The Biological Bulletin* 159(2): 269–279.
Hayward BW, Cedhagen T, Kaminski M et al. (2017) World foraminifera database. Available at: http://www.marinespecies. org/foraminifera/aphia.
Hearty PJ, O'Leary MJ, Kaufman DS et al. (2004) Amino acid geochronology of individual foraminifer (*Pulleniatina obliquiloculata*) tests, north Queensland margin, Australia: A new approach to correlating and dating quaternary tropical marine sediment cores. *Paleoceanography* 19(4): 1–14.
Heaton TJ, Köhler P, Butzin M et al. (2020) Marine20—The marine radiocarbon age calibration curve (0–55,000 cal BP). *Radiocarbon* 62: 779–820.
Hepp DA, Romero OE, Mörz T et al. (2019) How a river sub- merges into the sea: A geological record of changing a fluvial to a marine paleoenvironment during early Holocene sea level rise. *Journal of Quaternary Science* 34(7): 581–592.
Hijma MP, Cohen KM, Hoffmann G et al. (2009) From river valley to estuary: The evolution of the Rhine mouth in the early to middle Holocene (western Netherlands, Rhine-Meuse delta). *Netherlands Journal of Geosciences* 88(1): 13–53.
Horne DJ and Boomer I (2000) The role of Ostracoda in salt- marsh meiofaunal communities. In: Sherwood BR, Gardiner BG and Harris T (eds) *British Saltmarshes*. London: Linnean Society, pp.181–202.
Kaufman D (2006) Temperature sensitivity of aspartic and glutamic acid racemization in the foraminifera Pulleniatina. *Quaternary Geochronology* 1(3): 188–207.
Kaufman DS (2000) Amino acid racemization in ostracodes. In: Goodfriend G, Collins M, Fogel M et al. (eds) *Perspectives in Amino Acid and Protein Geochemistry*. New York, NY: Oxford University Press, pp.145–160.
Kaufman DS and Manley WF (1998) A new procedure for deter- mining DL amino acid ratios in fossils using reverse phase liquid chromatography. *Quaternary Science Reviews* 17(11): 987–1000.
Kowalke T (2006) History of mollusc community types and fau- nal dynamics in continental saline ecosystems of the south Mediterranean quaternary. *Rivista Italiana di Paleontologia e Stratigrafia* 112(2): 275.
Lachenal AM (1989) Ecologie des ostracodes du domaine medi- terranéen: application au Golfe de Gabes (Tunisie Orientale). Les variations au niveau marin depuis 30.000 ans. *Documents des Laboratoires de Géologie de Lyon* 108: 238.
Lepoint G, Cox AS, Dauby P et al. (2006) Food sources of two detritivore amphipods associated with the seagrassPosidonia oceanicaleaf litter. *Marine Biology Research* 2(5): 355–365.
Lin J (1990) Mud crab predation on ribbed mussels in salt marshes. *Marine Biology* 107(1): 103–109.
Loeblich AR and Tappan H (1988) *Foraminiferal Genera and Their Classification*. New York, NY: Van Nostrand Reinhold Company.
McGlathery K, Sundbäck K and Anderson I (2007) Eutrophication in shallow coastal bays and lagoons: The role of plants in the coastal filter. *Marine Ecology Progress Series* 348: 1–18.
Maddocks RF (1966) Distribution patterns of living and subfossil podocopid ostracodes in the Nosy Be area, northern Mada- gascar. *University of Kansas Paleontological Contributions* 12: 72.
Maddocks RF (1969) Recent ostracodes of the family Pontocypri- didae chiefly from the Indian Ocean. *Smithsonian Contributions to Zoology* 7: 1–56.
Maher BA (1998) Magnetic properties of modern soils and qua- ternary loessic paleosols: Paleoclimatic implications. *Palaeogeography, Palaeoclimatology, Palaeoecology* 137(1–2): 25–54.
Manteca JI, Ros-Sala M, Ramallo-Asensio S et al. (2017) Early metal pollution in southwestern Europe: The former littoral lagoon of el Almarjal (Cartagena mining district, S.E. Spain). A sedimentary archive more than 8000 years old. *Environmental Science and Pollution Research* 24: 10584–10603.
Manteca Martínez JI and García García C (2004) La falla de Cartagena-La Unión. Aportación a su conocimiento y verificación visual de su existencia gracias a una obra pública. *Actas V Reunión Comisión Patrimonio Geológico de la Sociedad Geológica de España*, pp.239–246.
Manteca Martínez JI and Ovejero Zappino G (1992) Los yacimientos Zn, Pb, Ag-Fe del distrito

minero de La Unión- Cartagena, Bética Oriental. *Recursos Minerales de España. CSIC. Col Textos Universitarios* 15: 1085–1102.
Marriner N and Morhange C (2006) The 'Ancient Harbour Parasequence': Anthropogenic forcing of the stratigraphic highstand record. *Sedimentary Geology* 186(1–2): 13–17.
Marriner N and Morhange C (2007) Geoscience of ancient Medi- terranean harbours. *Earth-Science Reviews* 80: 137–194.
Marriner N, Morhange C, Doumet-Serhal C et al. (2006) Geosci- ence rediscovers Phoenicia's buried harbors. *Geology* 34: 1–4. Marriner N, Morhange C, Kaniewski D et al. (2014) Ancient harbour infrastructure in the Levant: Tracking the birth and rise of new forms of anthropogenic pressure. *Scientific Reports* 4(1): 5554.
Martín-Puertas C, Jiménez-Espejo F, Martínez-Ruiz F et al. (2010) Late Holocene climate variability in the southwestern Mediterranean region: An integrated marine and terrestrial geochemical approach. *Climate of the Past* 6: 807–816.
Martínez-García B, Pascual A, Rodríguez-Lázaro J et al. (2013) The Ostracoda (Crustacea) of the Tina Menor estuary (Canta- bria, southern Bay of Biscay): Distribution and ecology. *Journal of Sea Research* 83: 111–122.
Martinez-Ruiz F, Kastner M, Gallego-Torres D et al. (2015) Paleoclimate and paleoceanography over the past 20,000 yr in the Mediterranean Sea basins as indicated by sediment elemental proxies. *Quaternary Science Reviews* 107: 25–46.
Mazzella L, Scipione MB, Gambi MC et al. (1993) The Mediter- ranean seagrass Posidonia oceanica and Cymodocea nodosa: A comparative overview. In: Ozhaen E (ed.) *Proceedings of the First International Conference on the Mediterranean Coastal Environment*, vol. 93. pp.103–116.
Mazzini I, Anadon P, Barbieri M et al. (1999) Late quaternary sea-level changes along the Tyrrhenian coast near Orbetello (Tuscany, central Italy): Palaeoenvironmental reconstruction using ostracods. *Marine Micropaleontology* 37: 289–311.
Meisch C (2000) Crustacea: Ostracoda. In: Schwoerbel J and Zwick P (eds) *Süßwasserfauna von Mitteleuropa 8/3*. Heidel- berg: Spektrum Akademischer Verlag, 522 pp.
Melis RT, Di Rita F, French C et al. (2018) 8000 years of coastal changes on a western Mediterranean island: A multiproxy approach from the Posada plain of Sardinia. *Marine Geology* 403: 93–108.
Menier D, Tessier B, Proust JN et al. (2010) The Holocene trans- gression as recorded by incised-valley infilling in a rocky coast context with low sediment supply (southern Brittany, western France). *Bulletin de la Société Géologique de France* 181: 115–128.
Milker Y and Schmiedl G (2012) A taxonomic guide to modern benthic shelf foraminifera of the western Mediterranean Sea. *Palaeontologia Electronica* 15: 1–134.
Morhange C, Goiran JP, Bourcier M et al. (2000) Recent Holo- cene paleo-environmental evolution and coastline changes of Kition, Larnaca, Cyprus, Mediterranean Sea. *Marine Geology* 170(1–2): 205–230.
Morhange C and Marriner N (2010a) Paleo-hazards in the coastal Mediterranean: A geoarchaeological approach. In: Martini IP and Chesworth P (eds) *Landscapes and Societies*. Dordrecht: Springer, pp.223–234.
Morhange C and Marriner N (2010b) Mind the (stratigraphic) gap: Roman dredging in ancient Mediterranean harbours. *Bollettino di Archeologia on line* 1: 23–32.
Morhange C, Marriner N and Carayon N (2016) The eco-history of ancient Mediterranean harbours. In: Bekker-Nielsen T and Gertwagen R (eds) *The Inland Seas, Towards an Ecohistory of the Mediterranean and the Black Sea*. Stuttgart: Franz Steiner Verlag, pp.85–107.
Morhange C, Pirazzoli PA, Evelpidou N et al. (2012) Late Holocene tectonic uplift and the silting up of Lechaion, the west- ern harbor of ancient Corinth, Greece. *Geoarchaeology* 27(3): 278–283.
Murdock KJ, Wilkie K and Brown LL (2013) Rock magnetic properties, magnetic susceptibility, and organic geochemistry comparison in core LZ1029-7 Lake El'gygytgyn, Russia Far East. *Climate of the Past* 9: 467–479.
Murray-Wallace CV (1995) Aminostratigraphy of quaternary coastal sequences in southern Australia—An overview. *Qua- ternary International* 26: 69–86.

Murray-Wallace CV and Goede A (1995) Aminostratigraphy and electron spin resonance dating of quaternary coastal neotecto- nism in Tasmania and the Bass Strait islands. *Australian Journal of Earth Sciences* 42(1): 51–67.

Nachite D, Rodríguez-Lázaro J, Martín-Rubio M et al. (2010) Distribution et écologie des associations d'ostracodes récents de l'estuaire de Tahadart (Maroc Nord-Occidental). *Revue de Micropaleontologie* 53: 3–15.

Navarro-Hervás F, Ros-Salas MM, Rodríguez-Estrella T et al. (2014) Evaporite evidence of a mid-Holocene (c. 4550–4400 cal. yr BP) aridity crisis in southwestern Europe and palaeoenvironmental consequences. *The Holocene* 24(4): 489–502.

Nieto-Moreno V, Martínez-Ruiz F, Giralt S et al. (2011) Tracking climate variability in the western Mediterranean during the late Holocene: A multiproxy approach. *Climate of the Past* 7: 1395–1414.

Nieto-Moreno V, Martinez-Ruiz F, Giralt S et al. (2013) Climate imprints during the 'Medieval Climate Anomaly' and the 'Little Ice Age' in marine records from the Alboran Sea basin. *The Holocene* 23: 1227–1237.

Nijenhuis IA, Becker J and De Lange GJ (2001) Geochemistry of coeval marine sediments in Mediterranean ODP cores and a land section: Implications for sapropel formation models. *Palaeogeography, Palaeoclimatology, Palaeoecology* 165(1– 2): 97–112.

Nowaczyk NR, Frank U, Mingram J et al. (2004) The contribution of high-resolution magnetostratigraphic analyses to paleoclimatic reconstructions. In: Fischer H, Kumke T, Lohmann G et al. (eds) *The Climate in Historical Times: Towards a Synthesis of Holocene Proxy Data*. Heidelberg: Springer-Verlag Berlin, pp.351–363.

Oen IS, Fernandez JC and Manteca JI (1975) The lead-zinc and associated ores of La Union, Sierra de Cartagena, Spain. *Economic Geology* 70: 1259–1278.

Ortega B, Caballero M, Lozano S et al. (2006) Rock magnetic and geochemical proxies for iron mineral diagenesis in a tropical lake: Lago Verde, Los Tuxtlas, East–Central Mexico. *Earth and Planetary Science Letters* 250: 444–458.

Ortiz JE, Torres T, Julià R et al. (2004a) Algoritmos de cálculo de edad a partir de relaciones de racemización/epimerización de aminoácidos en pelecípodos marinos del litoral mediterráneo español. *Revista de la Sociedad Geológica de España* 17(3–4): 217–227.

Ortiz JE, Torres T, Julià R et al. (2004b) Numerical dating algorithms of amino acid racemization ratios from continental ostra- codes. Application to the Guadix-Baza Basin (southern Spain). *Quaternary Science Reviews* 23(5–6): 717–730.

Ortiz JE, Torres T, López-Cilla I et al. (2021) Keys to discern the Phoenician, Punic and Roman mining in a typical coastal environment through the multivariate study of trace element distribution. *The Science of the Total Environment* 790: 147986.

Ortiz JE, Torres T and Pérez-González A (2013) Amino acid racemization in four species of ostracodes: Taxonomic, environmental, and microstructural controls. *Quaternary Geochronology* 16: 129–143.

Ortiz JE, Torres T, Ramallo SF et al. (2015) Algoritmos de datación por racemización de aminoácidos de ostrácodos del Holoceno y Pleistoceno superior en la Península Ibérica. *Geogaceta* 58: 59–62.

Ortiz JE, Torres T, Sánchez-Palencia Y et al. (2022) Lipid bio- markers and metal pollution in the Holocene record of Cartagena Bay (SE Spain): Coupled natural and human induced environmental history in Punic and Roman times. *Environmental Pollution* 297: 118775.

Pedersen TF and Price NB (1980) The geochemistry of iodine and bromine in sediments of the Panama Basin. *Journal of Marine Research* 38(3): 397–411.

Pérez-Crespo MT (1992) *El Arsenal de Cartagena en el S. XVIII*. Madrid: Naval.

Pint A and Frenzel P (2017) Ostracod fauna associated with Cyprideis torosa– An overview. *Journal of Micropalaeontology* 36: 113–119.

Ramallo SF and Berrocal MC (1994) Mineria púnica y romana en el sureste peninsular: el foco de Carthago Nova. In: Vaquer- izo D (ed.) *Minería y metalurgia en la España prerromana y romana. Área de Cultura de la Excelentísima Diputación Provincial de Córdoba*. Córdoba: Servicio de Publicaciones, pp.79–146.

Raynal O, Bouchette F, Certain R et al. (2010) Holocene evolution of a Languedocian lagoonal environment controlled by inherited coastal morphology (northern Gulf of Lions, France). *Bulletin de la Société Géologique de France* 181(2): 211–224.
Reimer PJ, Austin WEN, Bard E et al. (2020) The IntCal20 North- ern Hemisphere radiocarbon age calibration curve (0–55 cal kBP). *Radiocarbon* 62: 725–757.
Richards GW (1985) Fossil Mediterranean molluscs as sea-level indicators. *Geological Magazine* 122: 373–381.
Robinson SG, Maslin MA and McCave IN (1995) Magnetic susceptibility variations in upper Pleistocene deep-sea sediments of the NE Atlantic: Implications for ice rafting and paleo-circulation at the last glacial maximum. *Paleoceanography* 10(2): 221–250.
Rodríguez-Estrella T, Navarro F, Ros M et al. (2011) Holocene morphogenesis along a tectonically unstable coastline in the western Mediterranean (SE Spain). *Quaternary International* 243(1): 231–248.
Rossi F, Colao E, Martinez MJ et al. (2013) Spatial distribution and nutritional requirements of the endosymbiont-bearing bivalve *Loripes lacteus* (sensu Poli, 1791) in a Mediterranean *Nanozostera noltii* (Hornemann) meadow. *Journal of Experi- mental Marine Biology and Ecology* 440: 108–115.
Rossi V and Vaiani SC (2008) Benthic foraminiferal evidence of sediment supply changes and fluvial drainage reorganization in Holocene deposits of the Po Delta, Italy. *Marine Micropaleontology* 69(2): 106–118.
Rovere A, Stocchi P and Vacchi M (2016) Eustatic and relative sea level changes. *Current Climate Change Reports* 2(4): 221–231.
Rowntree KM, van der Waal BW and Pulley S (2017) Magnetic susceptibility as a simple tracer for fluvial sediment source ascription during storm events. *Journal of Environmental Management* 194: 54–62.
Ruiz F, González-Regalado ML, Baceta JI et al. (2000a) Los ostrácodos actuales de la laguna de Venecia (NE de Italia). *Geobios* 33: 447–454.
Ruiz F, González-Regalado ML, Menegazzo L et al. (2000b) Los ostrácodos de la Cuenca del Lido (Laguna de Venecia, NE Italia). *Geogaceta* 27: 151–154.
Ruiz F, González-Regalado ML, Muñoz JM et al. (2003) Population age structure techniques and ostracods: Applications in coastal hydrodynamics and paleoenvironmental analysis. *Palaeogeography, Palaeoclimatology, Palaeoecology* 199: 51–69.
Sakellariou D and Galanidou N (2016) Pleistocene submerged landscapes and palaeolithic archaeology in the tectonically active Aegean region. *Geological Society* 411(1): 145– 178.
Saxena S (2005) *Text Book of Mollusca*. New Delhi: Discovery Publishing house.
Sciuto F, Rosso A, Sanfilippo R et al. (2015) Ostracods from mid- outer shelf bottoms of the Ciclopi Islands marine protected area (Ionian Sea, eastern Sicily). *Bollettino della Società Paleontologica Italiana* 54(2): 1–15.
Sisma-Ventura G, Antonioli F, Silenzi S et al. (2020) Assessing vermetid reefs as indicators of past sea levels in the Mediter- ranean. *Marine Geology* 429: 106313.
Smith AJ and Horne DJ (2002) Ecology of marine, marginal marine and nonmarine ostracodes. In: Holmes JA and Chi- vas AR (eds) *The Ostracode: Applications in Quaternary Research*. Washington, DC: American Geophysical Union, pp.37–64.
Soriano J, López-Salgado J, Quiñonero S et al. (2010) Primera cita de *Eastonia rugosa* (Helbling, 1799) (Bivalvia: Mactri- dae) en las costas catalanas. *SPIRA* 3: 197–200.
Spellerberg IF and Fedor PJ (2003) A tribute to Claude Shan- non (1916-2001) and a plea for more rigorous use of species richness, species diversity and the 'Shannon-Wiener' index. *Global Ecology and Biogeography* 12(3): 177–179.
Stefaniuk L, Morhange C, Blanc PF et al. (2005) Évolution des paysages littoraux dans la dépression sud-ouest de Cumes depuis 4000 ans. La question du port antique. *Méditerranée* 104: 49–59.
Stone JR, Cronin TM, Brewster-Wingard GL et al. (2000) A paleoecologic reconstruction of the history of Featherbed Bank, Biscayne National Park, Biscayne Bay, Florida. USGS, Open-File report 00-191: 1–24.
Stuiver M, Reimer PJ and Reimer RW (2021) CALIB 8.2 [WWW program]. Available at:

http://calib.org (accessed 7 December 2021).
Szczechura J (2006) Middle Miocene (Badenian) ostracods and green algae (Chlorophyta) from Kamienica Nawojowska, Nowy Sącz Basin (Western Carpathians, Poland). *Geologica Carpathica* 57: 103–122.
Tomasello A, Perrone R, Colombo P et al. (2018) Root hair anatomy and morphology in *Posidonia oceanica* (L.) Delile and substratum typology: First observations of a spiral form. *Aquatic Botany* 145: 45–48.
Torres T, Ortiz JE, Ros M et al. (2019) *Reflejo estratigráfico de los forzamientos climáticos, neotectónicos y antrópicos en el paleopaisaje de la bahía de Mazarrón (Murcia)*. XV Reunión Nacional del Cuaternario, pp.83–86.
Torres T, Ortiz JE, Sánchez-Palencia Y et al. (2020a) The Pleistocene and Holocene records of the Mazarrón Basin (SE Spain). *Quaternary International* 566: 256–270.
Torres T, Ortiz JE, Sánchez-Palencia Y et al. (2020b) El registro cuaternario sumergido de la Bahía de Cartagena (Murcia, España. *Geogaceta* 67: 27–30.
Torres T, Ramallo S, Sánchez-Palencia Y et al. (2018) Recon- structing human–landscape interactions in the ancient Medi- terranean harbour of Cartagena (Spain). *The Holocene* 28(6): 879–894.
Triantaphyllou MV, Kouli K, Tsourou T et al. (2010) Paleoenvironmental changes since 3000 BC in the coastal marsh of Vravron (Attica SE Greece). *Quaternary International* 216: 14–22.
Trincherini PR, Domergue C, Manteca I et al. (2009) The identi- fication of lead ingots from the Roman mines of Cartagena: The rôle of lead isotope analysis. *Journal of Roman Archaeology* 22: 123–145.
Urra J, Mateo Ramírez Á, Marina P et al. (2013) Highly diverse molluscan assemblages of *Posidonia oceanica* meadows in northwestern Alboran Sea (W Mediterranean): Seasonal dynamics and environmental drivers. *Estuarine, Coastal and Shelf Science* 117: 136–147.
Uzunova S (2010) The zoobenthos of the eelgrass populations from Sozopol Bay (Black Sea). *Bulgarian Journal of Agricultural Science* 16: 358–363.
Vacchi M, Ghilardi M, Melis RT et al. (2018) New relative sea- level insights into the isostatic history of the western Mediter- ranean. *Quaternary Science Reviews* 201: 396–408.
Vacchi M, Marriner N, Morhange C et al. (2016) Multiproxy assessment of Holocene relative sea-level changes in the western Mediterranean: Sea-level variability and improvements in the definition of the isostatic signal. *Earth-Science Reviews* 155: 172–197.
Vis GJ, Bohncke SJP, Schneider H et al. (2010) Holocene flooding history of the lower Tagus valley (Portugal). *Journal of Quaternary Science* 25(8): 1222–1238.
Vis GJ, Kasse C and Vandenberghe J (2008) Late Pleistocene and Holocene palaeogeography of the lower Tagus Valley (Portugal): Effects of relative sea level, valley morphology and sediment supply. *Quaternary Science Reviews* 27(17–18): 1682–1709.
Walker M, Head MJ, Berkelhammer M et al. (2018) Formal ratification of the subdivision of the Holocene Series/Epoch (Qua- ternary System/Period): Two new global boundary stratotype sections and points (GSSPs) and three new stages/subseries. *Episodes* 41: 213–223.
Walker MJC, Berkelhammer M, Björck S et al. (2012) Formal subdivision of the Holocene series/epoch: A discussion paper by a Working Group of INTIMATE (integration of ice-core, marine and terrestrial records) and the Subcommission on Quaternary Stratigraphy (International Commission on Stratigraphy). *Journal of Quaternary Science* 27(7): 649–659.
Walne PR and Dean GJ (1972) Experiments on predation by the shore crab, Carcinus maenas L., on Mytilus and Mercenaria. *ICES Journal of Marine Science* 34(2): 190–199.
Warning B and Brumsack HJ (2000) Trace metal signatures of eastern Mediterranean sapropels. *Palaeogeography, Palaeoclimatology, Palaeoecology* 158(3–4): 293–309.
Wehausen R and Brumsack HJ (1999) Cyclic variations in the chemical composition of eastern Mediterranean Pliocene sed- iments: A key for understanding sapropel formation. *Marine Geology* 153(1–4): 161–176.
Yim WWS, Huang G and Chan LS (2004) Magnetic susceptibil- ity study of late quaternary inner continental shelf sediments in the Hong Kong SAR, China. *Quaternary International* 117(1): 41–54.

Ziegler M, Jilbert T, de Lange GJ et al. (2008) Bromine counts from XRF scanning as an estimate of the marine organic carbon content of sediment cores. *Geochemistry Geophysics Geosystems* 9(5): Q05009.

Zilhão J, Angelucci DE, Badal-García E et al. (2010) Symbolic use of marine shells and mineral pigments by Iberian Nean- derthals. *Proceedings of the National Academy of Sciences of the United States of America* 107: 1023–1028.

Zuschin M and Gützer C (2014) Molluscan life and death assem- blages of a sheltered lagoon in the northern Red Sea: Implications for paleoecology, regional. *Geophysical Research Abstracts* 16: EGU2014-9606.